Far East J. Appl. Math. **25**(1) (2006), 73-84

PULSATILE FLOW IN A STENOSED RIGHT CORONARY ARTERY

BIYUE LIU

Department of Mathematics
Monmouth University
West Long Branch, NJ 07764, U. S. A.

Abstract

We present a three dimensional model with simplified geometry for a diseased right coronary artery segment to study the blood flow in a stenosed coronary artery and to understand the influence of the artery geometry on the flow pattern. The system of unsteady incompressible Navier Stokes equations is employed as the governing equation. The model is numerically solved using the finite element method. Computations are carried out under a variety of physiological flow conditions to examine the disturbed flow patterns, including flow shift, reverse flow, secondary flow and wall shear stress, in a curved artery with a stenosis at the inner wall of the bend at different stages through a cardiac cycle.

I. Introduction

Atherosclerosis is the leading cause of mortality in the western country. It is widely believed that the development of atherosclerosis is closely related to the complex haemodynamics in human arterial system. More and more clinical and research findings suggest that biomechanical factors such as flow velocity, wall shear stress and static pressure may be responsible for the formation and progression of atherosclerosis [2, 5, 10].

2000 Mathematics Subject Classification: 76D05, 92C50, 76M10.

Keywords and phrases: right coronary artery, atherosclerosis, blood flow, wall shear stress, finite element.

Received May 9, 2006

Atherosclerosis preferentially occurs in certain regions such as the bend and bifurcation of large and medium arteries. The local vascular geometry substantially mediates the haemodynamic environment of the intima [4]. The disturbed flow field with low and oscillating wall shear stress and fluctuated pressure in these regions are believed to contribute to the preferential occurrence of atherosclerotic plaque in these regions [5, 10]. Therefore, it is very important to study the blood flow in arteries with bends and bifurcations in order to understand the biomedical pathophysiology of atherosclerosis.

The coronary artery is a common and important clinical site of atherosclerotic plaque formation. Many studies have been made towards understanding the haemodynamics in coronary arteries [1, 5, 6, 8, 9, 14]. He et al. studied the blood flow in a left coronary artery bifurcation [8]. Back et al. examined the effect of mild atherosclerosis on flow resistance in a coronary artery casting of man [1]. Myers et al. investigated the effect of flow waveform and inlet velocity profile on the haemodynamics in the proximal, medial and distal arterial regions [12]. Johnston et al. compared the models of Newtonian and Non-Newtonian flows in healthy right coronary arteries with no sign of atheroma [9]. Despite the fact that the blood flow in coronary arteries has been intensively studied, the complex correlation between the haemodynamics in the coronary artery and atherosclerosis is still not fully understood. Further fluid dynamical and artery geometrical studies are needed.

The aim of the present study is to numerically analyze the local flow information in a portion of stenosed right coronary artery. Numerical computations are carried out under a variety of physiological flow conditions to investigate the local flow in curved arteries with a stenosis at the inner wall of the bend. The disturbed flow patterns at different stages in a cardiac cycle are examined.

II. Mathematical Model and Numerical Methods

This study assumes that the fluid is Laminar, Newtonian, viscous and incompressible and the artery wall is rigid. These assumptions have been shown to be adequate for arterial haemodynamics by many investigators [3, 8, 9, 16]. The unsteady three-dimensional Navier Stokes equations are

used to describe the blood flow in a portion of right coronary arteries as shown in Fig. 1. In the case of a stenosed artery, the geometry of the artery was reconstructed based on the image of a diseased artery in Figure 5 in [15] regarding the location, size and the shape of the stenosis. It consists of three parts. The first part is a straight 1.0 cm long inlet tube, followed by a curved second part which is initially obtained by rotating the end-cross-section of the first part by an angle of 72° with a 1.8 cm radius of curvature. The third part is a straight outlet tube following the curved part. The artery has circular cross sections with a 0.45 cm diameter at both inlet and outlet and with varying diameters in the region of stenosis. The area of the cross section at the throat of stenosis is reduced by 51%. In each cross section of the artery there is one diameter that connects the top point (outer wall) and the bottom point (inner wall) of the circle. We refer to this diameter as the center diameter.

The Navier Stokes equations are complemented with the following boundary conditions. The no-slip condition is imposed on the wall of artery. At the inlet boundary of artery, a blunt inlet velocity profile with a time varying waveform is assumed. $u = U(t)f(r)$, where r is the radial distance of a point to the center of the cross section circle. The value of f is zero for $r = 0.255\,\text{cm}$ and 1 for $r < 0.17\text{cm}$, and continuously varies between 0 and 1 for $0.17\,\text{cm} < r < 0.225\,\text{cm}$. Fig. 2(a) is a plot of this blunt profile along the normalized center diameter. $U(t)$, as shown in Fig. 2(b), is the pulsatile coronary inlet velocity waveform [1, 9, 11]. This physiological profile was recorded in the right coronary artery of a human and contains a period of reverse flow in systole and a rapid acceleration and deceleration in diastole. The outlet boundary is a circular cross-section perpendicular to the main axis of the tube. The surface traction free boundary condition is imposed at this boundary [12, 13, 17]. In computation the density of the fluid ρ is chosen as 1.05g/cm^3 and the dynamic viscosity η is chosen as 0.0245dynes/cm^2. The mean reference Reynolds number at the inlet is 348.

The Navier Stokes equations are solved numerically using the finite element method with piecewise quadratic functions for velocity and piecewise linear functions for pressure over a tetrahedral mesh. The

computations are performed using COMSOL software (version 3.2). The initial conditions for velocity and pressure are obtained by solving the steady state Navier Stokes equations with the same boundary conditions as in the time dependent problem. A few cycles are simulated to ensure that the flow is truly periodic. Computations are repeated and compared over different meshes to ensure that the numerical solutions are mesh independent.

III. Observations and Conclusion

Simulation results are analyzed to investigate the flow pattern in a segment of right coronary artery with a stenosis at the inner wall and the influence of the stenosis on the flow. The flow pattern varies at different stages during the cardiac cycle. The solution at four representative times $(t = 0.05, 0.1, 0.3, 0.85\text{s})$ is demonstrated. As marked in Fig. 2(b), they correspond to a systolic deceleration with a forward inlet velocity $(t = 0.05\text{s})$ and a reverse inlet velocity $(t = 0.1\text{s})$, a systolic acceleration $(t = 0.3\text{s})$ and the point of maximum forward velocity in diastole $(t = 0.85\text{s})$. It is well known that an irregular flow field caused by the curvature occurs at the inner wall of a bend. However, with the presence of a stenosis at the inner wall, the flow at the inner wall in the region of post-stenosis becomes more irregular and a disturbed flow region also occurs at the outer wall of downstream.

Flow shift and reverse flow

Fig. 3 shows a representative data set of axial velocity along the normalized center diameter at the time values of 0.05, 0.1, 0.3 and 0.85s through the cardiac cycle at different cross sections ci $(i = 1, 2, ..., 6)$ of the artery. The center diameter is a diameter of a cross section circle in the plan of curvature. $x = 0$ and $x = 1$ correspond to the outer wall and the inner wall respectively. c1 is a cross section near the entry of the artery; c2 is at the end of the straight inlet tube; c3 is in the middle of the curved part; c4 is immediately below the stenosis; c5 is in the downstream; c6 is near the outlet boundary. In the plot a positive axial velocity means the fluid moves forward and a negative axial velocity indicates the fluid moves backward. The flow separation pattern in a

curved artery with stenosis can be observed in Fig. 3. When t = 0.05s nearly blunt forward flow is observed near the entry of the inlet (see c1 in Fig. 3a). At the end of the straight inlet tube, backward flows are observed near both outer wall and inner wall. As the fluid moves into the curved part and downstream, the maximum forward axial velocity shifts towards the outer wall and the backward flow near the inner wall further develops and the flow separation at the inner wall reaches the maximum in the post-stenosis region. As the fluid moves further down, the maximum forward axial velocity shifts back to the center of the tube and the backward flow at the inner wall is weakened. It is interesting to compare the axial velocity plots in Fig. 3(a) and Fig. 3(b). The axial velocity curves at each cross section for t = 0.05s and t = 0.1s have similar shapes except near the entry of the inlet. This suggests that the reverse flow and flow shifting patterns in the curved artery when t = 0.05s and t = 0.1s (both in decelerations during the systole) are similar despite the fact that the velocity waveform at the inlet is backward when t = 0.1s.

Fig. 3(c) shows that, when t = 0.3s, the axial velocity profile keeps nearly blunt along the artery except in the post-stenosis region where it becomes nearly parabolic. No backward flow is observed. From Fig. 3(d) we can see that at the peak of the diastole (t = 0.85s), there is no significant flow shifting in the straight inlet tube and the first half of the curved part. The maximum forward axial velocity shifts towards the outer wall and a flow separation occurs at the inner wall in the post-stenosis. The maximum reverse flow is on the order of 20% in magnitude compared to the forward flow in the cross section. As the fluid moves to the outlet the flow separation disappears and the axial velocity profile resumes a regular shape with the maximum at the center.

Fig. 4 is a plot of streamline of the velocity field when t = 0.05, 0.1, 0.3, 0.85s respectively. It shows that during the systolic deceleration with a small forward or backward inlet velocity the flow along the artery is irregular in the curved part and post-stenosis region, especially at the inner wall of the post-stenosis when t = 0.05s and at the outer wall of downstream when t = 0.1s. During the systolic acceleration, flow is more regular and there is no sign of flow shifting and reverse flow. The last plot

of streamline in Fig. 4 shows a shifted flow towards the outer wall and a flow recirculation at the inner wall of the post-stenosis region when $t = 0.85$s.

Secondary flow

Secondary flows occur along the curved arteries as a result of acting centrifugal forces. The pattern of the secondary flow in a stenotic curved artery is more complex than that in a curved artery with no stenosis. The magnitude of the secondary flow in a stenotic curved artery is also much larger. An approach to assessing the secondary flow is to examine the maximum magnitude of the transverse velocity on each cross section along the artery. Fig. 5(a) is a plot of the maximum axial velocity magnitude and the maximum transverse velocity magnitude on each cross section along the artery when $t = 0.85$s. The transverse velocity contains the velocity components perpendicular to the axial velocity. The horizontal axis is the normalized axial length of the artery. $x = 0$ and $x = 1$ correspond to the inlet and outlet boundary respectively. The straight inlet tube is between $x = 0$ and $x = 0.17$. The throat of the stenosis is at $x = 0.34$ and the end of the stenosis is at $x = 0.41$. Fig. 5(a) demonstrates that the maximum axial velocity assumes the maximum at the cross section with $x = 0.41$ which is below the stenosis. The maximum secondary flow occurs at the cross section with $x = 0.34$ which is the throat of the stenosis. Fig. 5(b) is the ratio of the maximum secondary flow to the maximum axial velocity on each cross section. This ratio assumes the maximum value 0.31 at the middle of the curved part ($x = 0.3$). It indicates that the secondary flow is strongest at the middle of the curved part which is on the order of 31% to the axial velocity.

Wall shear stress

Fig. 6 and Fig. 7 show the wall shear stress distributions (in dyne/cm^2) at the time values of 0.05, 0.1, 0.3 and 0.85s respectively during the cardiac cycle in a curved artery with 51% stenosis and with no stenosis, respectively. Negative wall shear stresses indicate a reverse flow. From Fig. 6 and Fig. 7 we can see that the pattern of wall shear stress in a curved artery with a stenosis at the inner wall is more complex than that in an artery with no stenosis. During the systolic deceleration,

the low wall shear stress region occurs at the inner wall of the middle of the curve part and the high wall shear stress occurs at the outer wall of the second half of the curved part in a curved artery with no stenosis. However in a curved artery with 51% stenosis, there are two intense regions of low wall shear stress at the inner wall, one in the second half of the curved part and the other in the downstream of the post-stenosis region. Regions of fairly low wall shear stress also exist at the inner wall towards the outlet. High wall shear stress occurs at the outer wall of post-stenosis region. It is believed that low wall shear stress and blood stagnation increase residence time and interaction between blood lipoproteins and vessel endothelium. This may result in the thickening of the arterial vessel wall [5, 7]. During the systolic acceleration, no negative wall shear stress is observed regardless the presence of stenosis and a relatively low wall shear stress region occurs in the post-stenosis region in a stenosed artery (Fig. 6(c)). At the peak velocity of diastole, the wall shear stress in the second half of the curved part is very high compared to the values of the wall shear stress at other times in the cardiac cycle.

The comparison between the wall shear stress in Fig. 6 and Fig. 7 also clearly demonstrates that the difference between the maximum and minimum values of the wall shear stress at each time value is much larger in a curved artery with stenosis than that in an artery with no stenosis.

In conclusion, in the pulsatile arterial flow field in a curved artery with stenosis, two low wall shear stress regions at the inner wall are observed during the systolic deceleration. The region distal to the stenosis is characterized by a reverse flow and low wall shear stress at the inner wall, a maximum flow shifting and strong secondary flow. These phenomena in flow can contribute to abnormal pathologic mechanisms which may promote further development of the atherosclerotic plaque.

Acknowledgements

This work was supported, in part, by a grant-in-aid for Creativity Award from Monmouth University.

References

[1] L. H. Back, Y. I. Cho, D. W. Crawford and R. F. Cuffel, Effect of mild atherosclerosis on flow resistance in a coronary artery casting of man, Trans. ASME 106 (1984), 48-53.

[2] C. G. Caro, J. M. Fitz-Gerald and R. C. Schroter, Atheroma and arterial wall shear observation, correlation and proposal of a shear-dependent mass transfer mechanism for atherogenesis, Proc. Roy. Soc. London 177 (1971), 109-159.

[3] D. D. Duncan, C. B. Bargeron and S. E. Borchardt, The effect of compliance on wall shear in cast of a human aortic bifurcation, ASME J. Biomech. Engg. 112 (1990), 183-188.

[4] M. H. Friedman, O. J. Deters, F. F. Mark, C. B. Bargeron and G. M. Hutchins, Geometric effects on the hemodynamic environment of arterial wall: a basis for geometric risk factors?, Fluid Dynamics as a Localizing Factor for Atherosclerosis, G. Schettler, R. M. Nerem, H. Schmid-Schonbein, H. Morl and C. Diehm, eds., Springer, Berlin, 1983, pp. 71-78.

[5] G. D. Giannoglou, J. V. Soulis, T. M. Farmakis, D. M. Farmakis and G. E. Louridas, Haemodynamic factors and the important role of local low static pressure in coronary wall thickening, Int. J. Cardiology 86 (2002), 27-40.

[6] C. M. Gibson, L. Diaz, K. Kandarpa, F. M. Sacks et al., Relation of vessel wall shear stress to atherosclerosis progression in human coronary arteries, Arteriosclerosis and Thrombosis 13 (1993), 310-315.

[7] S. Glagov, C. Zarins, D. P. Giddens and D. N. Ku, Hemodynamics and atherosclerosis. Insights and perspectives gained from studies of human arteries, Arch. Pathol. Lab. Med. 112 (1988), 1018-1031.

[8] X. He and D. N. Ku, Pulsatile flow in the human left coronary artery bifurcation: Average conditions, Trans. ASME 118 (1996), 74-82.

[9] B. M. Johnston, P. R. Johnston, S. Corney and D. Kilpatrick, Non-Newtonian blood flow in human right coronary arteries: Transient simulations, J. Biomech. 39 (2005), 1116-1128.

[10] D. N. Ku, D. P. Giddens, C. K. Zarins and S. Glagov, Pulsatile flow and atherosclerosis in the human carotid bifurcation: Positive correlation between plaque location and low and oscillating stress, Arteriosclerosis 5 (1985), 292-302.

[11] S. Matsuo, M. Tsuruta, M. Hayano, Y. Immamura, Y. Eguchi, T. Tokushima and S. Tsuji, Phasic coronary artery flow velocity determined by Doppler flowmeter catheter in aortic stenosis and aortic regurgitation, Amer. J. Cardiology 62 (1988), 917-922.

[12] J. G. Myers, J. A. Moore, M. Ojha, K. W. Johnston and C. R. Ethier, Factors influencing blood flow patterns in the human right coronary artery, Ann. Biomed. Engg. 29 (2001), 109-120.

[13] G. Pedrizzetti and K. Perktold, Cardiovascular Fluid Mechanics, courses and lectures, no. 446, p. 78, Springer, New York, 2003.

[14] M. Prosi, K. Perktold, Z. Ding and M. H. Friedman, Influence of curvature dynamics on pulsatile coronary artery flow in a realistic bifurcation model, J. Biomech. 37 (2004), 1767-1775.

[15] H. N. Sabbah, F. Khaja, J. F. Brymer, E. T. Hawkins and P. D. Stein, Blood flow in the coronary arteries of man: relation to atherosclerosis, Blood Flow in Large Arteries: Applications to Atherogenesis and Clinical Medicine, D. W. Liepsch, ed., Monographs on Atherosclerosis, Vol. 15, pp. 77-90, Basel, Karger, 1990.

[16] D. A. Steinman and C. R. Ethier, Numerical modeling of flow in a dispensable end-to-side anastomosis, BED, Bioengineering Conference, ASME 24 (1993), 379-382.

[17] X. Y. Xu and M. W. Collins, Haemodynamics of Arterial Organs, Comparison of Computational Predictions with In vitro and In Vivo Data, pp. 49, WIT Press, 1999.

(a) (b)

Figure 1. A curved artery with a 72° angle of bend.
(a) with no stenosis, (b) with a 51% stenosis.

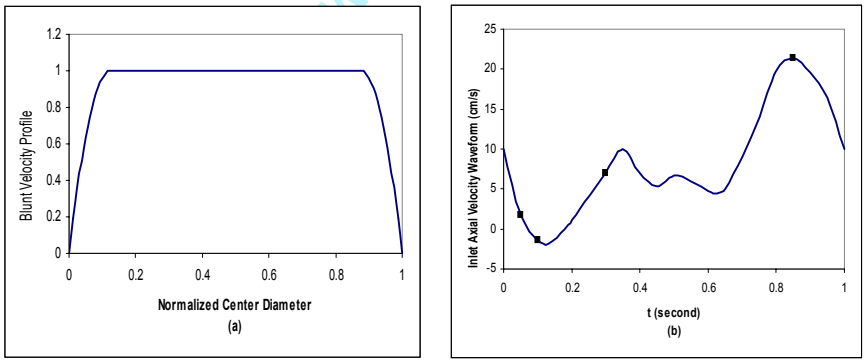

Figure 2. (a) Blunt velocity profile at inlet boundary,
(b) Pulsatile coronary inlet velocity waveform.

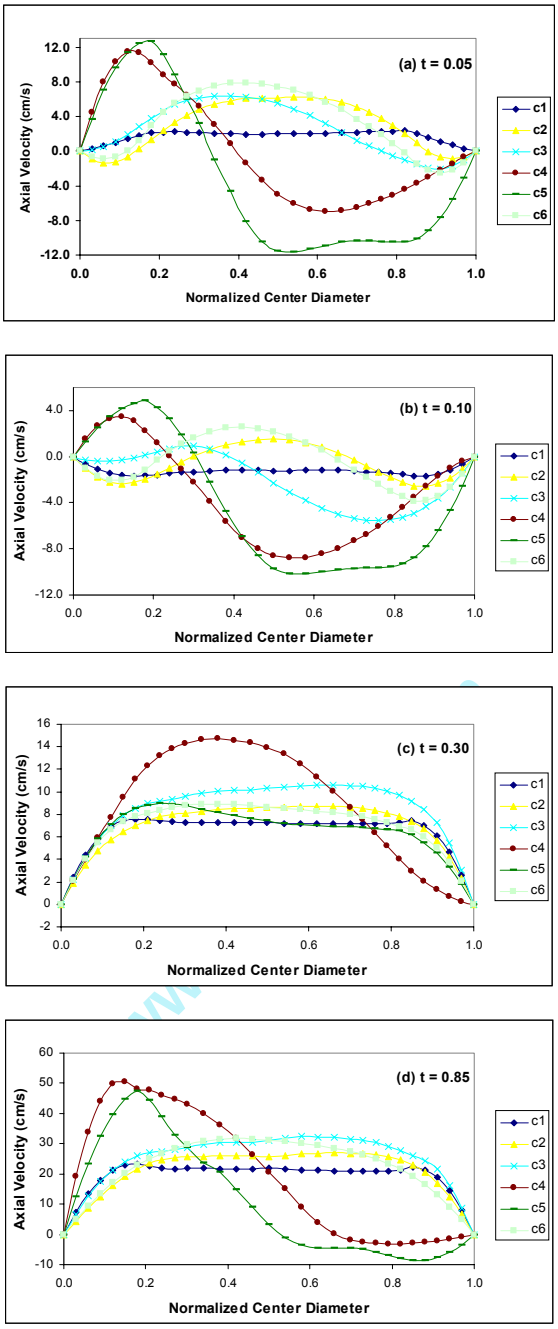

Figure 3. Axial velocity along normalized center diameter at t = 0.05s(a), 0.1s(b), 0.3s(c), 0.85s(d).

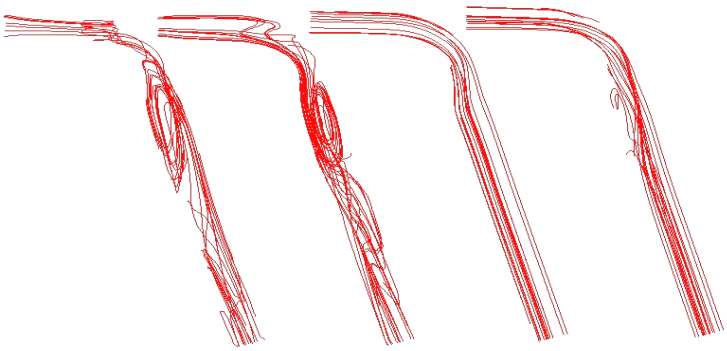

Figure 4. Streamline of the velocity field at t = 0.05s, 0.1s, 0.3s, 0.85s.

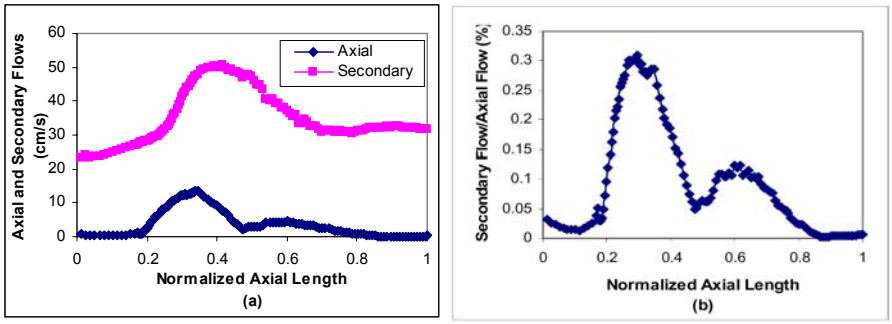

Figure 5. (a) Maximum axial velocity and maximum secondary flow on each cross section along the artery, (b) Percent of the secondary flow visas axial velocity.

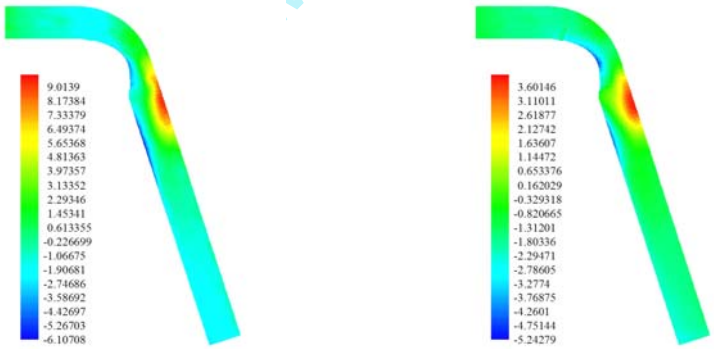

(a) (b)

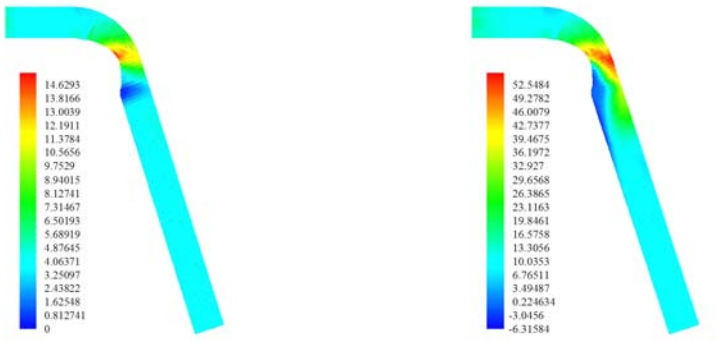

(c) (d)

Figure 6. Wall shear stress distribution (a) t = 0.05s, (b) t = 0.1s, (c) t = 0.3s, (d) t = 0.85s in a curved artery with 51% stenosis.

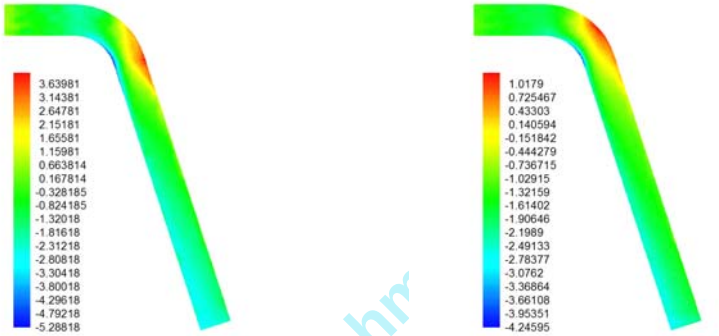

(a) (b)

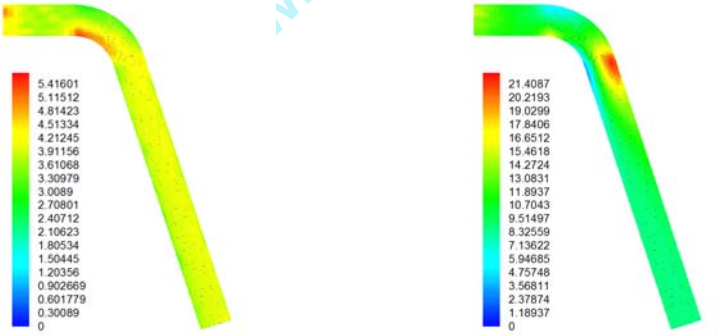

(c) (d)

Figure 7. Wall shear stress distribution (a) t = 0.05s, (b) t = 0.1s, (c) t = 0.03s, (d) t = 0.85s, in a curved artery with no stenosis.